JACS
JOURNAL OF THE AMERICAN CHEMICAL SOCIETY

ARTICLE

pubs.acs.org/JACS

# Temperature Dependent Equilibrium Native to Unfolded Protein Dynamics and Properties Observed with IR Absorption and 2D IR Vibrational Echo Experiments

Jean K. Chung,[†] Megan C. Thielges,[†] Sarah E. J. Bowman,[‡] Kara L. Bren,[‡] and M. D. Fayer*[,†]

[†]Department of Chemistry, Stanford University, Stanford, California 94305, United States

[‡]Department of Chemistry, University of Rochester, Rochester, New York 14627, United States

Supporting Information

**ABSTRACT:** Dynamic and structural properties of carbonmonoxy (CO)-coordinated cytochrome $c_{552}$ from *Hydrogenobacter thermophilus* (*Ht*-M61A) at different temperatures under thermal equilibrium conditions were studied with infrared absorption spectroscopy and ultrafast two-dimensional infrared (2D IR) vibrational echo experiments using the heme-bound CO as the vibrational probe. Depending on the temperature, the stretching mode of CO shows two distinct bands corresponding to the native and unfolded proteins. As the temperature is increased from low temperature, a new absorption band for the unfolded protein grows in and the native band decreases in amplitude. Both the temperature-dependent circular dichroism and the IR absorption area ratio $R_A(T)$, defined as the ratio of the area under the unfolded band to the sum of the areas of the native and unfolded bands, suggest a two-state transition from the native to the unfolded protein. However, it is found that the absorption spectrum of the unfolded protein increases its inhomogeneous line width and the center frequency shifts as the temperature is increased. The changes in line width and center frequency demonstrate that the unfolding does not follow simple two-state behavior. The temperature-dependent 2D IR vibrational echo experiments show that the fast dynamics of the native protein are virtually temperature independent. In contrast, the fast dynamics of the unfolded protein are slower than those of the native protein, and the unfolded protein fast dynamics and at least a portion of the slower dynamics of the unfolded protein change significantly, becoming faster as the temperature is raised. The temperature dependence of the absorption spectrum and the changes in dynamics measured with the 2D IR experiments confirm that the unfolded ensemble of conformers continuously changes its nature as unfolding proceeds, in contrast to the native state, which displays a temperature-independent distribution of structures.

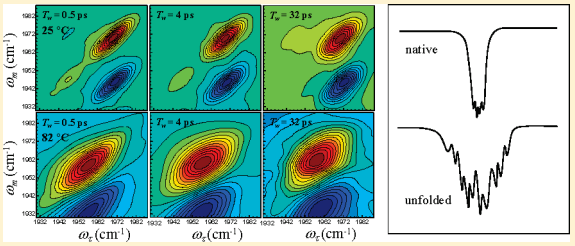


## I. INTRODUCTION

Understanding protein folding has been recognized as one of the most important problems in biology and biochemistry. Many experiments and theoretical studies on the structure and folding of proteins have been focused on the native structure rather than the unfolded state. This is not only due to the obvious relevance of the native state protein to its biological functions but also because of difficulties associated with characterizing proteins under unfolding conditions, where they can exist in heterogeneous distributions of many conformations.[1,2] The properties of unfolded proteins play crucial roles in folding and stability, transport across membranes, and proteolysis and protein turnover.[1]

With advances in analytical techniques such as multidimensional nuclear magnetic resonance,[3,4] hydrogen−deuterium exchange,[5] small-angle X-ray scattering,[6,7] fluorescence,[8] single molecule spectroscopy,[9] and time-resolved visible photon echo spectroscopy,[10] light has been shed on the characteristics of the unfolded state. Although it was once thought that when a protein denatures it becomes a random coil,[11] data using these new techniques, and theories developed along with them, have shown that in many cases proteins retain residual secondary and tertiary structure even under severely denaturing conditions.[1,7,12] Furthermore, studies have shown that mutations as well as varying denaturing conditions influence the nature of unfolded proteins. Because of its inherent heterogeneity, the ensemble of protein structures that exist in the unfolded state are described in terms of statistics.[13] The concept and language of energy landscapes, the notion that the protein can assume a large number of nearly isoenergetic conformations around local energy minima, are useful for describing the unfolded states and their dynamics.[14]

Owing to its availability, simplicity, robustness, and biological importance, the monomeric, globular, and water-soluble cytochrome *c* (cyt *c*) has been employed in many protein folding studies, both experimental[10,15,16] and theoretical.[17,18] In this study, we have used a mutated cyt $c_{552}$ from thermophilic bacteria, *Hydrogenobacter thermophilus* (cyt *c Ht*-M61A). The crystal structure of wild-type cyt *c Ht* is depicted in Figure 1.[19]

**Received:** December 18, 2010
**Published:** April 06, 2011

  

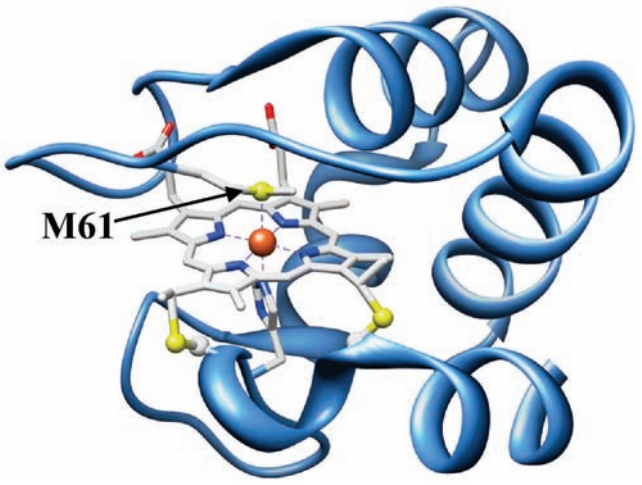


**Figure 1.** The crystal structure of wild-type cytochrome $c_{552}$ from *Hydrogenobacter thermophilus* (PDB 1YNR). The sulfur atom of Met61 occupies the sixth coordination site of the heme iron in the wild type. In the experiments, a Met61Ala mutation allowed the coordination of carbon monoxide in its place. The heme is covalently bound to the protein by two thioether linkages, tethering the vibrational probe to the protein even when it is unfolded.

The replacement of the axial methionine M61 by alanine allows the ligation of carbon monoxide (CO) to the heme-center iron.[20,21] The CO serves as the vibrational reporter in the infrared (IR) studies described here. *Ht*-M61A cyt *c* is very well suited for thermal unfolding experiments as it shows remarkable stability and reversibility under severe thermal denaturing conditions.[22−25] Also important is the fact that the prosthetic heme group, the site of the protein's functional activities and the location of the vibrational probe, is covalently bound to the protein via two thioether linkages (Figure 1). This ensures that the heme containing the vibrational probe does not dissociate from the protein upon denaturation. The stretching mode of the CO probe has been used in numerous IR studies in various heme proteins such as myoglobin, hemoglobin, horseradish peroxidase, and cytochrome P450, due to its exquisite sensitivity to the local environment and the strong vibrational signal it produces in a spectroscopic region in aqueous solution that has a relatively low water background absorption.[26]

In this paper, we describe experiments that examine the native protein and its unfolded states under equilibrium conditions at various temperatures using IR experiments. Time-independent linear IR absorption, as well as time-dependent ultrafast two-dimensional infrared (2D IR) vibrational echo spectroscopy, were employed to investigate the steady-state and ultrafast time scale behavior of the protein under increasingly severe thermal denaturing conditions. These IR methods have been established as sensitive tools for probing fast protein dynamics on time scales that are inaccessible by other techniques.[27,28] Previous studies using 2D IR vibrational echoes on heme proteins investigated the dynamics of native proteins,[28−30] enzyme−substrate interactions,[31,32] dynamic changes associated with various mutations,[33,34] switching between protein substates,[35] and chemical denaturation.[21]

The CO absorption spectrum of the native protein shows a single peak at room temperature. At the onset temperature for unfolding, a new band at lower frequency appears and grows in as the temperature is further increased. As the unfolded band grows in, the native band decreases in amplitude. The ratio, $R_A(T)$, area of the unfolded band divided by the sum of the areas of the native and unfolded bands plotted against temperature has an S shape that closely resembles the temperature dependent plot of the circular dichroism (CD) data. Both the IR area and the CD data can be fit to the standard two-state thermodynamic model.[36] However, the unfolded IR absorption band provides additional information. As the temperature is increased, the unfolded line width increases and the peak position shifts to lower frequency, but there are no changes in the width or position of the native band. The increase in line width of the unfolded peak is caused by increased inhomogeneous broadening as verified by the 2D IR spectroscopy. The increase in inhomogeneous line width demonstrates that the number of protein conformational structures grows as the temperature is elevated. This behavior is clearly not simple two-state unfolding.

2D IR vibrational echo spectroscopy measures spectral diffusion, that is, the time-dependent changes in the frequencies of the IR chromophores, which manifests as time-dependent changes in the shape of the 2D IR spectrum. Spectral diffusion is directly related to the time dependence of protein structural changes. These line shape changes are directly related to the frequency-frequency correlation function (FFCF), which yields information about the rate at which the protein samples different structural configurations. The FFCF separates the ultrafast dynamics into three regimes: motionally narrowed homogeneous dynamics, intermediate structural evolution (0.3 to ∼100 ps), and structural changes that are so slow that they are outside of the experimental time window (>100 ps). It was found that the homogeneous component is sensitive only to the temperature change and is independent of whether the protein is folded or unfolded. The longer time scale dynamics show distinct trends for the native versus unfolded configurations. The unfolded protein displays dynamics that become increasingly fast as the temperature increases. In contrast, the dynamics of the native state show no changes with temperature. Like the increase in the inhomogeneous line width of the unfolded absorption band, the increase in the rate of structural dynamics as the temperature increases demonstrates that the unfolded protein undergoes a continuous unfolding process. These findings are consistent with the concept of variable denatured states, which have been described theoretically and investigated experimentally.[1,37,38] The observed temperature dependence of the unfolded protein dynamics is not consistent with a simple two-state model.

## II. METHODS

**A. Sample Preparation.** *Ht*-M61A cyt $c_{552}$ was expressed in *E. coli* following procedures that have been described previously.[39] 2 mg of protein was dissolved in 3 M guanidine hydrochloride (GuHCl), 100 mM sodium phosphate (pD 7) in deuterium oxide ($D_2O$) to obtain a protein concentration of approximately 10 mM. GuHCl is necessary to prevent aggregation of the sample at higher temperatures and to give a fully denatured protein in the accessible temperature range. To ligate CO to the protein heme, 5 equiv of sodium dithionite were added to the protein solution to reduce the iron from Fe(III) to Fe(II), and the solution was stirred in a CO atmosphere for 20 min. The solution was left in the CO atmosphere for another 20 min to ensure the completion of the CO ligation. 30 $\mu$L of the sample was then pipetted onto a 3 mm thick calcium fluoride ($CaF_2$) window, and sandwiched by another window with a 50 $\mu$m thick Teflon spacer in between in a custom-built

copper sample cell. The optical density of the CO stretching band at 1973 $cm^{-1}$ was approximately 0.07.

Detailed tests were performed to demonstrate that aggregation of the protein did not occur at the experimental sample concentration of 10 mM over the full range of temperatures studied. The temperature-dependent IR absorption spectrum of the amide I band of the sample was monitored at 10 mM and at a lower concentration, 3 mM. The two samples were prepared identically as described above. Because of the strong amide I absorption, a sample path length of 6 $\mu$m was used. The aggregation of cyt *c* is known to cause peaks to grow at 1616 and 1685 $cm^{-1}$ due to the formation of intermolecular $\beta$-sheets.[40,41] No such peaks were detected in either the 3 or 10 mM samples over the full temperature range. Furthermore, there was no detectable difference between the small temperature-dependent spectral changes of the two samples. Therefore, protein aggregation does not occur. The temperature dependent spectra are shown in the Supporting Information.

**B. Infrared Absorption and Circular Dichroism Experiments.** For the temperature-dependent FT-IR and 2D IR experiments, a programmable resistive heater and silicon diode temperature sensor (Lakeshore D470) attached to the copper sample cell were used to control the temperature of the sample. To ensure the minimal thermal gradient across the sample, thermally conductive washers were placed between the cell and the calcium fluoride windows, which are also excellent heat conductors. The temperature of the sample reached equilibrium at a set point with fluctuations less than 0.2 °C. A series of FT-IR spectra were taken with Bruker Vertex 70 FT-IR spectrometer from 4 to 80 °C in 4 °C increments with 1 $cm^{-1}$ resolution. Prior to analysis, each spectrum was background-subtracted by fitting the solvent baseline. The resulting spectra usually showed a gentle sloping background due to the minute differences in water spectra. These backgrounds were removed with cubic spline fits. At the end of each experiment, the sample was brought down to room temperature and FT-IR spectra were taken that confirmed the reversibility of thermal unfolding.

Temperature-dependent CD measurements required a careful sample preparation. Because sodium dithionite absorbs strongly at 222 nm resulting in saturation of the signal, dithiothreitol (DTT) was used as the reducing agent instead. To avoid the oxidation of cyt *c* during experiment, the solvent was degassed in inert gas to remove oxygen and CO-bound cyt *c* (20 $\mu$M in 100 mM sodium phosphate, pD 7.0, 3.0 M GuHCl) was prepared in a wet glovebox. The sample was loaded into a gastight 2-mm path length quartz cell. UV−vis spectra of the CO-bound heme absorption were checked before and after the experiment to make sure no oxidation had occurred. The CD (Jasco J810) signal at 222 nm was recorded at every 5 °C from 25 to 80 °C.

**C. Two Dimensional Infrared (2D IR) Vibrational Echo Spectroscopy.** The experimental methods for heterodyned 2D IR spectroscopy are described in full detail elsewhere.[27,42,43] The output of a Ti:Sapphire oscillator is regeneratively amplified in a Ti:Sapphire regenerative amplifier. The resulting 1 kHz, 800 nm, 100 fs pulses are subsequently converted into mid-infrared pulses in an optical parametric amplifier. This conversion process produces 120 fs, 5 $\mu$J pulses at a 1 kHz repetition rate at the experimental wavelength of ~1960 $cm^{-1}$. The bandwidth of the pulse is sufficiently broad, ~120 $cm^{-1}$, to cover the 0−1 vibrational transitions of the native and unfolded bands as well as their 1−2 transitions.

Briefly, the 2D IR vibrational echo experiments involve application of three mid-IR light pulses with wave vectors $k_1$, $k_2$, and $k_3$ to the sample in a boxcar geometry, with the times between the first and second pulse and the second and third pulse referred to as $\tau$ and $T_w$, respectively.[42] At a time $\leq \tau$ after the third pulse, a vibrational echo is emitted by the sample in the phase-matching $(-k_1 + k_2 + k_3)$ direction. The vibrational echo pulse is overlapped with another IR pulse, called the local oscillator, which provides a phase reference for the vibrational echo signal. The combined vibrational echo/local oscillator pulse is passed through a monochromator onto an IR array detector, which records a spectrum that yields the $\omega_m$ frequency axis (vertical axis), the axis of vibrational echo emission. Scanning $\tau$ produces an interferogram at each $\omega_m$. These interferograms are Fourier transformed to produce the second, $\omega_\tau$ axis (horizontal axis), of the 2D IR spectrum.

In the experiments, $\tau$ is scanned for fixed $T_w$ (time between pulses 2 and 3) to produce a 2D IR spectrum. $T_w$ is then changed, and $\tau$ is again scanned to produce another 2D IR spectrum. The change in the spectra with $T_w$ provides the dynamical information about the system.

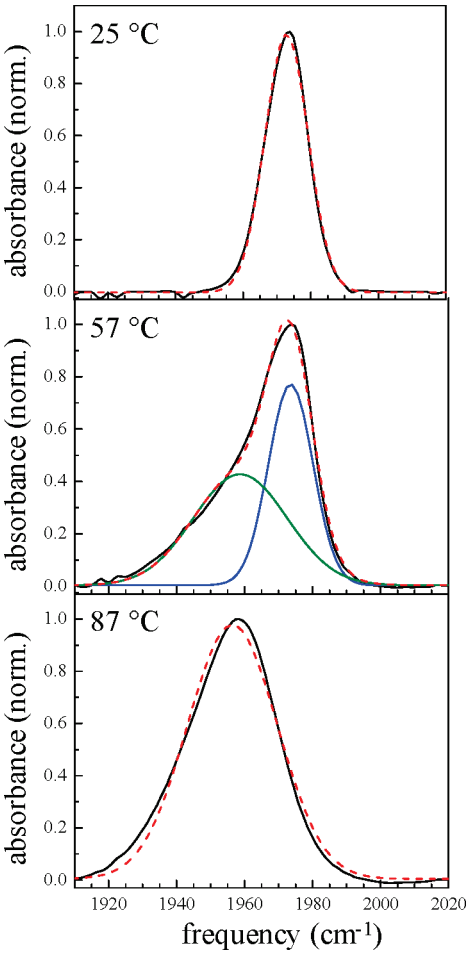


**Figure 2.** FT-IR spectra of CO-bound cyt *c Ht*-M61A at 25 °C (native protein), at 57 °C (overlapping bands of the native and unfolded protein), and 87 °C (unfolded protein) in 3 M GuHCl, 100 mM sodium phosphate, $D_2O$, pD 7. The black curves are the data. The dashed red curves are Gaussian fits to the data. In the middle panel, the spectrum was fit to the sum of two Gaussian bands. The blue (native) and green (unfolded) curves are the two Gaussians that result from the fit.

## III. RESULTS

**A. Time-Independent Spectroscopy.** A series of FT-IR spectra of the stretching mode of CO bound to cyt *c* in 3 M GuHCl were taken between 4 and 85 °C. Figure 2 displays FT-IR spectra at three temperatures. In the lower temperature range (4 to 30 °C), the spectrum is a single Gaussian band at 1973 $cm^{-1}$ with a full width at half-maximum (fwhm) of 15 $cm^{-1}$. This is the spectrum of CO when the protein is known to have the native structure,[3,21] so we designate this band the


dx.doi.org/10.1021/ja111009s |J. Am. Chem. Soc. 2011, 133, 6681–6691

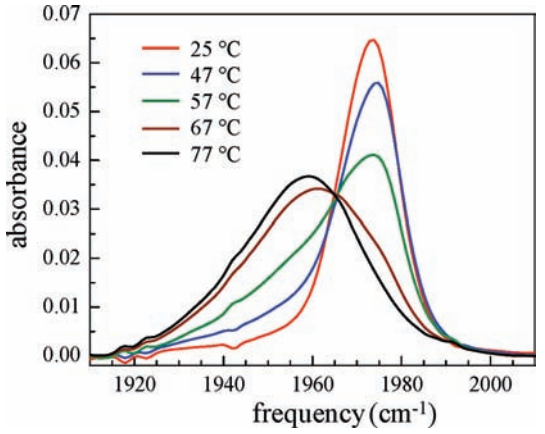


**Figure 3.** FT-IR spectra at different temperatures showing the progression of the absorption spectrum from low temperature (native protein) to high (unfolded protein) and the isosbestic point.

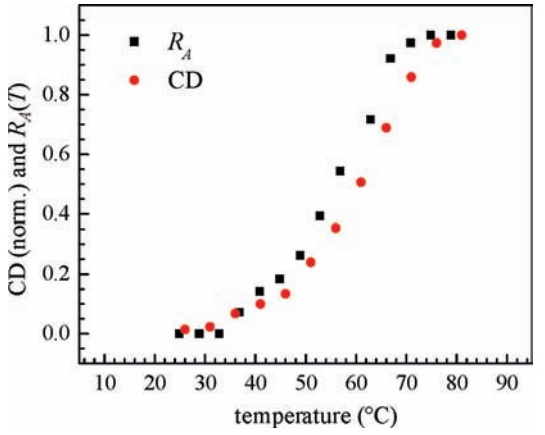


**Figure 4.** Comparison between temperature dependent CD signal at 222 nm (normalized) and the FT-IR band area ratio, $R_A$. $R_A$ is the ratio of the area of the unfolded band to the sum of the areas of the native and unfolded bands. Both types of data give the appearance of two-state protein unfolding. The transition temperatures ($T_m$) are 56 ± 2 and 60 ± 4 °C for $R_A$ and CD, respectively.

"native band." When the temperature is raised further, another Gaussian band appears at a lower frequency. As cyt *c* is known to be unfolded at higher temperatures,[44] the lower frequency band is assigned as the spectrum of CO when cyt *c* is no longer in the native configuration but has assumed an unfolded conformation. This band is referred to as the "unfolded band," although as discussed below, this band changes as the temperature is increased. The middle panel of Figure 2 shows the spectrum when both the native and unfolded bands are present. The native (blue) and unfolded (green) curves are the two Gaussians that comprise the fit. The bottom panel of Figure 2 shows the high temperature spectrum, where the native band has been reduced to essentially zero amplitude and the single band is the spectrum of the unfolded protein.

Figure 3 shows the progression of the change in the spectrum with temperature. At 25 °C, the spectrum is the single Gaussian native band. At 47 °C, a shoulder appears on the low frequency side of the predominately native band. By 57 °C, there is significant amplitude in the unfolded band as evidenced by the large tail to lower frequency. At 67 °C, the spectrum is dominated by the unfolded band with a high frequency shoulder due to the remaining native band. At 77 °C, the spectrum is essentially composed only of the unfolded band centered at 1958 $cm^{-1}$ with fwhm of 32 $cm^{-1}$.

The ratio $R_A(T)$ of the population of the unfolded state to the sum of the populations of the native and unfolded states at each temperature can be obtained from the temperature dependence of the areas of the IR absorption two bands.

$$R_A(T) = \frac{A_{uf}(T)}{A_n(T) + A_{uf}(T)} \quad (1)$$

where $A_{uf}$ is the area of the unfolded band, and $A_n$ is the area of the native band. As displayed in Figure 3, as the temperature is increased, $A_{uf}$ increases and $A_n$ decreases. At low temperature the ratio is 0 and at high temperature it is 1. It was found that sum of the areas, $A_n(T)+A_{uf}(T)$, is constant over the full temperature range within experimental error, demonstrating that the oscillator strength is conserved, and the ratio is the true ratio of the unfolded population to the total population. When $R_A(T)$ = 0.5, the populations of the native and unfolded ensembles are equal.

Figure 4 displays the $R_A(T)$ data and temperature dependent CD data. The CD data has been normalized for comparison to the $R_A(T)$ data. The two curves are almost the same. The transition temperatures ($T_m$) are 56 ± 2 °C and 60 ± 4 °C for $R_A$ and CD, respectively. (The difference in the two curves might be caused by a small systematic error. The volume of the sample used for the vibrational spectra measurements is very small. A slight loss of water during the sample preparation would increase the GuHCl concentration, moving the $R_A$ curve to lower temperature.)

The results displayed in Figure 4 are important for a number of reasons. The similarity between the CD data and the area ratio data shows that the IR absorption spectrum is sensitive to the protein unfolding in essentially the same manner as CD. It is assumed, in interpreting a CD curve such as the one shown in Figure 4, that the midpoint of the change corresponds to the point at which the native and unfolded protein ensembles are equally populated. The area ratio data gives an absolute measure of the populations.

The S-shaped curve (Figure 4) and the presence of an isosbestic point (Figure 3) are signatures of a cooperative 2-state transition.[36,45,46] However, this does not necessarily indicate a well-defined transition over a single free energy barrier, as many different types of more complicated transitions may show sigmoidal transition profiles that are indistinguishable without additional thermodynamic measurements.[1]

The CO stretching mode spectrum of the protein in the native state is a Gaussian band with peak frequency of 1973 $cm^{-1}$ and fwhm of 15 $cm^{-1}$. As shown in Figures 5A and C, when the temperature is raised, neither the center frequency nor the width changes; only the native band's amplitude decreases as the population in the native state moves to the unfolded state. The inhomogeneously broadened native band reflects a large distribution of structures that give rise to a range of CO stretching frequencies. The lack of a temperature dependence of the native absorption band and the results of the 2D IR studies discussed below demonstrate that native cyt *c* does not undergo structural changes as the temperature is increased. Its secondary and tertiary structures are maintained and the distribution of structures that give rise to the inhomogeneous absorption line is either

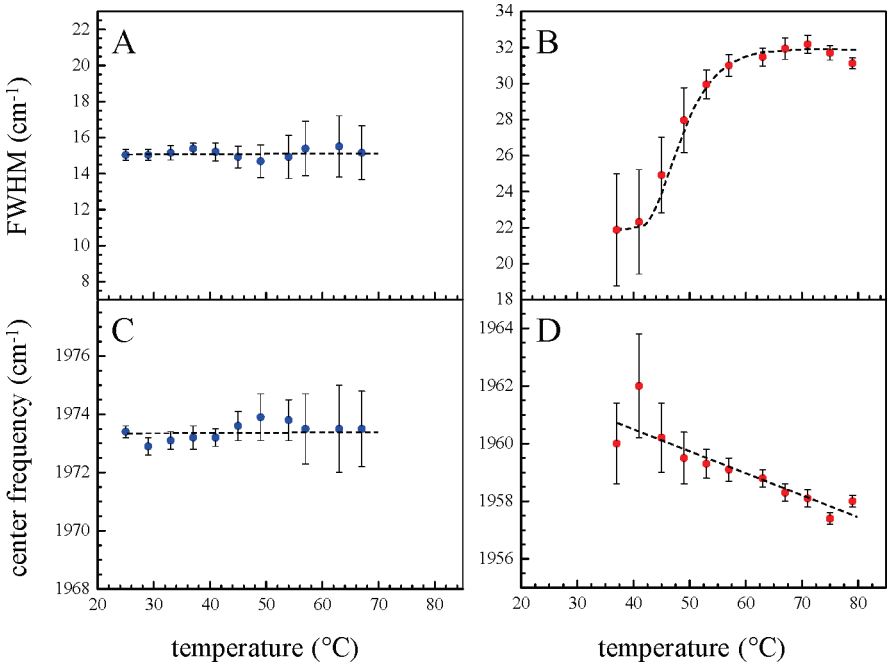


**Figure 5.** Temperature dependence of the line width of (A) the native peak and (B) the unfolded peak of the protein CO spectrum. The increase in width of the unfolded spectra with increasing temperature is caused by an increase in the inhomogeneous contribution, which results from an increase in the number of protein structures. The change in width with temperature demonstrates that the temperature dependent unfolding is not a two state process. Temperature dependence of the center frequency for the (C) native and (D) unfolded peaks, respectively. As with the fwhm, the native peak frequency shows little change, but the unfolded peak displays a discernible dependence on temperature. The error bars are from the errors in fitting the spectra at each temperature. Because there is only a small population of the native protein (blue points) at higher temperatures, the error bars are larger. Conversely, data for the unfolded protein (red points) have larger error bars at lower temperatures.

unchanged or changes very little as long as the protein does not unfold. The lack of temperature dependence is consistent with the idea that the distribution of native protein conformations occurs on an energy landscape that is relatively narrow around a deep local minimum. An increase in temperature does not enable the protein to access significantly different conformations of the folded protein.

The unfolded band displays a fundamentally different temperature-dependent behavior. The unfolded band can first be observed at 37 °C, at which temperature it has become large enough to be discernible at a lower frequency than the much larger native band. At this temperature, the unfolded band is centered at ~1961 $cm^{-1}$ and has a 22 $cm^{-1}$ fwhm. In contrast to the native band, both the line width and line center of the unfolded band are temperature dependent. As the temperature is increased, the unfolded band broadens and shifts to lower frequency; at 77 °C, the band is located at 1958 $cm^{-1}$ and has a fwhm of 32 $cm^{-1}$. The temperature dependence of the unfolded band line width is shown in Figure 5B and its center frequency is shown in Figure 5D. The change in the unfolded line width with increasing temperature is substantial. Comparing the native and unfolded forms at the lowest temperature where the unfolded line width can be measured, the difference in width is 7 $cm^{-1}$. As the temperature is increased, the unfolded line broadens another 10 $cm^{-1}$. Thus the increase in line width of the unfolded state with increasing temperature is greater than the initial increase in going from native to unfolded. The change in the center frequency is not as great, but clearly discernible.

The increase in the line width and the shift in the center frequency with increasing temperature demonstrate that unfolding is not a strict two-state process. The fact that the inhomogeneous line width of the unfolded band increases demonstrates that the number of conformations that are thermally accessible is increasing as the temperature increases. The average structure and distribution of structures are dependent on unfolding conditions (temperature), resulting in the band's red shift and line broadening. The line broadening and frequency shift also imply that the lower temperature unfolded states are not the random coils but have structures that change with increasing temperature. It is known that cyt *c* can adopt fairly compact conformations, smaller than expected for random coils under thermally denaturing conditions.[1,37] Thus, at a given temperature the unfolded state of cyt *c* consists of an ensemble of many protein conformations with a certain average structure and variance from the average. When the temperature is increased, the variance increases as shown by the increase in the inhomogeneous line width. The average structure also changes, which results in the band's red shift.

The CD data and the FT-IR area ratio data shown in Figure 3 suggest that both techniques report on the same particular change in structure that we will refer to as the primary unfolding event. The near coincidence of the transitions indicates that the growth of the unfolded band in the IR spectrum is associated with the same change in cyt c that leads to loss of helical structure. The IR spectra also provide information that cannot be obtained from the CD curve. The native and unfolded states manifest themselves as distinct peaks in the IR spectrum, and the unfolding can be monitored by the transfer of area between the two bands. Unlike the CD spectra, the IR spectra enable this scenario to be differentiated from another possibility that the protein changes in a continuous manner from native to unfolded. Had this occurred,


dx.doi.org/10.1021/ja111009s |*J. Am. Chem. Soc.* 2011, 133, 6681–6691

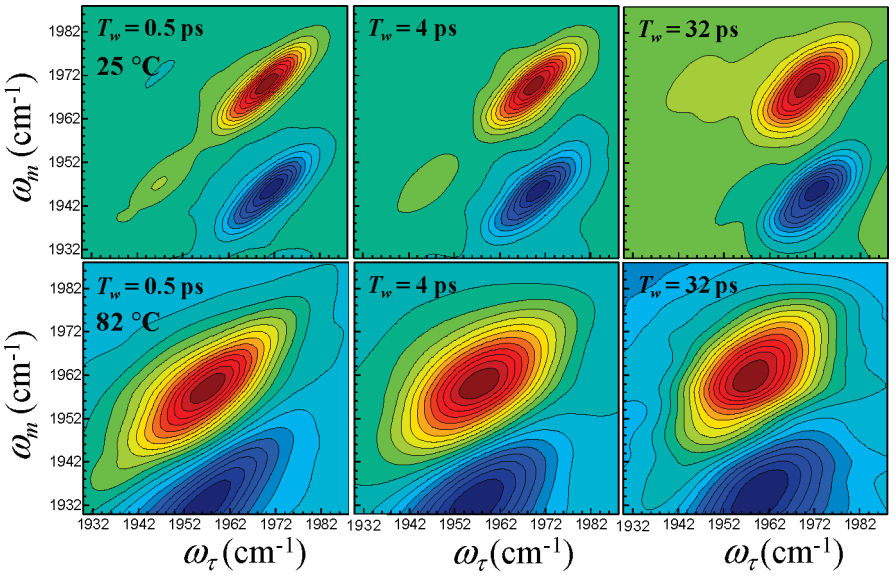


**Figure 6.** 2D IR vibrational echo spectra at three waiting times, $T_w$. The top panels are spectra from the native protein at 25 °C. The bottom panels are spectra from the unfolded protein at 82 °C. The change in shape of the spectra with increasing $T_w$ provides dynamical information.

the native band might continuously shift to the red and broaden as temperature is increased. This behavior would suggest continuous small changes in structure that influence the CO absorption frequency. The fact that a new, distinct band grows in indicates that the primary unfolding event is associated with significant structural changes that expose the CO to an environment dramatically different from the native state, leading to the abrupt change in the frequency of the CO absorption.

Extensive point mutation and other studies have shown that the interaction of heme iron-bound CO with a polar group shifts the center frequency of CO to lower frequency.[26,47] Consider myoglobin-CO (MbCO) which has three distinct CO absorption bands called $A_0$, $A_1$, and $A_3$.[48] These bands have frequencies of 1965, 1944, and 1939 cm$^{-1}$, respectively, for bovine heart MbCO. The difference in the frequencies is determined by the conformation of the imidazole side group of the distal histidine (H64). The $A_0$ band has the imidazole swung out of the pocket,[28] whereas both $A_1$ and $A_3$ have the imidazole in the pocket. $A_1$ has the imidazole protonated epsilon nitrogen ($N_\varepsilon H$) pointed away from the CO, while $A_3$ has the $N_\varepsilon H$ point more toward the CO.[28,29] The three bands are caused by well-defined structural differences that have a strong influence on the CO. The $A_0$ band, which has the highest frequency, does not have the imidazole in the pocket, so there is no interaction between the CO and the $N_\varepsilon H$. The $A_1$ band is shifted to lower frequency by the interaction between the $N_\varepsilon H$ and the CO, and the $A_3$ band is shifted even further to the red by a stronger interaction CO-$N_\varepsilon H$ interaction. The broad distribution of protein structures gives rise to the inhomogeneous broadening of each band, but it is a specific interaction that produces distinct bands. A shift in the CO absorption frequency through direct interaction with the CO is also known to occur for *Ht*-M61A. The mutation in which Gln64 is replaced with Asn (Q64N) induces CO to interact with the polar side group of Asn, resulting in a 9 cm$^{-1}$ frequency shift to the red.[20]

In analogy with the three bands of MbCO, it seems reasonable to view the 12 cm$^{-1}$ red-shift of the unfolded band relative to the native band as being caused by the primary unfolding event that produces a structural change that has direct impact on the CO. It is also reasonable to postulate that such a change is caused by CO being exposed to a polar group of an amino acid or possibly water. The significant increase in inhomogeneous broadening of the unfolded line relative to the native band indicates a considerable increase in the number of protein conformations. The red-shift and broadening of the CO band bound to cyt *c* has been observed previously via chemical denaturation.[21]

**B. 2D IR Vibrational Echo Spectroscopy.** The theory, analysis, and interpretation of 2D IR vibrational echo spectroscopy are described in full detail elsewhere.[42,49] The interpretation of a 2D IR spectrum will be described here briefly. The vibrational echo signals are recorded by scanning $\tau$ at fixed $T_w$ to produce a 2D IR spectrum, as described in Section II.C. $T_w$ is then increased, and another spectrum is taken. The changes in the peak shapes with increasing $T_w$ are directly related to the structural evolution of the protein as sensed by the CO. The first and second pulses label the initial frequencies of the CO vibrations, which have a range of frequencies because the ensemble of proteins is composed of a range of structures. Between the second and third pulses, structural evolution causes the initially labeled frequencies to change, a phenomenon known as spectral diffusion. The third pulse ends the evolution period, and the vibrational echo signal reads out the final frequencies of the initially frequency-labeled CO vibrations. As $T_w$ increases, there is more time for structural evolution to occur, so there are larger frequency changes.

Figure 6 shows 2D IR vibrational echo spectra collected at three $T_w$'s and two temperatures. The upper panels show 2D IR spectra for the protein in its native structure (25 °C), and the bottom panels show 2D IR spectra for the unfolded protein (82 °C). In each spectrum there are two dominant bands, positive and negative. The positive band (red) arises from the ground to first excited state (0−1) vibrational transition of the CO stretching mode, and the off-diagonal and negative (blue) band arises from vibrational echo emission at the first to second excited state transition frequency (1−2).[50−52] The negative off-diagonal bands are shifted to lower frequency along the $\omega_m$ axis


dx.doi.org/10.1021/ja111009s |*J. Am. Chem. Soc.* 2011, 133, 6681–6691

by the anharmonicity of the vibrational potential. Since the 0−1 and 1−2 bands provide the same information, only the 0−1 band was analyzed. In the first upper panel there are also two small bands, one on the diagonal at ($\omega_\tau$ = 1948 cm$^{-1}$, $\omega_m$ = 1948 cm$^{-1}$) that is positive, and one off-diagonal at (1948 cm$^{-1}$, 1972 cm$^{-1}$) that is negative. These arise from fifth order interactions, and do not influence the interpretation of the diagonal 0−1 bands.[53]

At short $T_w$ (0.5 ps), the bands in the 2D IR spectra show a strong elongation along the diagonal, a signature of inhomogeneous broadening. At short $T_w$, there are many structural configurations of the protein that have not yet been sampled by structural evolution. As time increases, structural evolution causes spectral diffusion, resulting in the change in shape of the 2D spectrum. The longest time for the measurements is limited by the vibrational lifetime of the CO stretching mode. In these experiments data could be collected to a maximum of 80 ps. The spectrum is sensitive to structural fluctuations that occur on a time scale up to a few times the longest $T_w$ measured because some portion of slower fluctuations will occur in the experimental window if their time scale is not too slow.[54] Looking at Figure 6, it is clear that at each $T_w$ the spectrum of the native protein is very different from that of the unfolded protein.

The frequency-frequency correlation function (FFCF) connects the $T_w$ dependent changes in the 2D band shapes caused by spectral diffusion to the time dependence of the structural changes of the proteins. The center line slope (CLS) method is used here to determine the FFCF from 2D and linear spectra.[49,55] This method provides an accurate way to extract the FFCF and also provides a useful quantity to plot for visualizing differences in the protein dynamics for different protein conformational states.[49,55] At a particular $\omega_\tau$, a slice through the 2D spectrum, projected onto the $\omega_m$ axis, is a one-dimensional spectrum with a peak at a particular $\omega_m$ value. Many such slices taken over a range of $\omega_\tau$ values produce a set of peak frequency points. Connecting the resulting points yields the center line. In the absence of a homogeneous contribution, at $T_w$ = 0, the 2D line shape is a line along the diagonal and the slope of the center line would be 1. At sufficiently long time, when spectral diffusion has sampled all frequencies, the 2D band is symmetric; the center line is horizontal with the slope of zero. It has been shown theoretically that the $T_w$-dependent part of the normalized FFCF is directly related to the $T_w$ dependence of the slope of the center line.[49,55] Thus the slope of the center line, the CLS, will vary between a maximum of 1 at $T_w$ = 0 and 0 in the limit of long waiting time. The $T_w$ = 0 slope will only be unity if there is no homogeneous contribution to the spectrum. The homogeneous contribution to the line shapes in the linear absorption and 2D spectra mainly comes from the motionally narrowed component produced by very fast structural fluctuations,[27,56,57] such that $\Delta\tau < 1$, where $\tau$ and $\Delta$ are the time constant and range (amplitude) of the frequency fluctuations. Other homogeneous contributions arise either from vibrational lifetime $T_1$, which is measured independently by IR pump−probe experiments, or from orientational relaxation, which can be neglected due to the large size, and therefore, very slow orientational relaxation of the protein. The homogeneous component of the spectrum causes the initial value of the slope to be less than 1 at $T_w$ = 0. The difference from 1 at $T_w$ = 0 combined with the $T_w$ dependent CLS and the linear absorption spectrum yields the full FFCF, including the $T_w$ independent homogeneous component.[49,55]

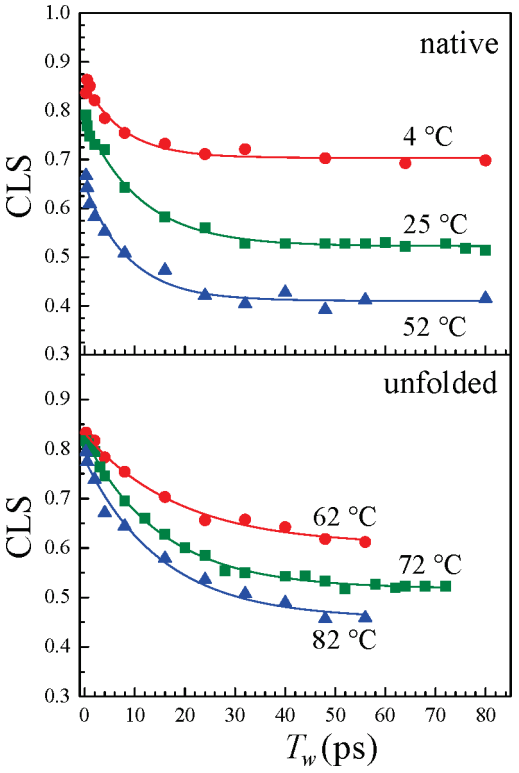


**Figure 7.** Center line slope (CLS) data (points) and fits (solid curves) for the native protein (top panel) and the unfolded protein (bottom panel) for several temperatures. The fits are to an exponential function with an offset.

The multiple time scale dynamics were modeled by a multi-exponential form of the FFCF, $C(t)$.

$$C(t) = \sum_{i=1}^{n} \Delta_i^2 e^{-t/\tau_i} + \Delta_s^2 \qquad (1)$$

The $\Delta_i$ and $\tau_i$ terms are amplitudes and correlation times, respectively, of the vibrational frequency fluctuations induced by protein structural dynamics. For the $i$th dynamical process, $\Delta_i$ is the range of CO frequencies sampled due to protein structural fluctuations, and $\tau_i$ is the time constant of these fluctuations. This form of the FFCF has been widely used and in particular found applicable in studies of the structural dynamics of heme-CO proteins.[21,27,28,30,31,33,34,58,59] Very slow structural fluctuations on time scales longer than the experimental time window are contained in the static term $\Delta_s^2$ in the FFCF. However for a motionally narrowed term with $\Delta_i\tau_i < 1$, these quantities cannot be evaluated separately; only the product $\Delta^2\tau = 1/T_2^*$, can be determined, where $T_2^*$ is the pure dephasing time. The homogeneous dephasing, which is determined from the analysis of the 2D IR spectra has a contribution from the vibrational lifetime, $T_1$, and the pure dephasing, $T_2^*$. The pure dephasing time is obtained by using $1/T_2 = 1/T_2^* + 1/2T_1$. $T_1$ is obtained from IR pump−probe experiments. The contribution to $T_2$ from the lifetime, ~0.25 cm$^{-1}$, is negligible at all but the lowest temperatures. The pure dephasing line width is $\Gamma = 1/\pi T_2^* = \Delta^2\tau$. In the data analysis presented below, the FFCF contains three terms, a homogeneous dephasing term given as $\Gamma$, a single exponential decay term $\Delta_1^2 e^{-t/\tau_1}$, and a static term, $\Delta_s^2$. $\Gamma$, $\Delta_1$, and $\Delta_s$ have a well-defined relationship to the absorption spectrum. $\Delta_1$ and $\Delta_s$


dx.doi.org/10.1021/ja111009s |J. Am. Chem. Soc. 2011, 133, 6681–6691

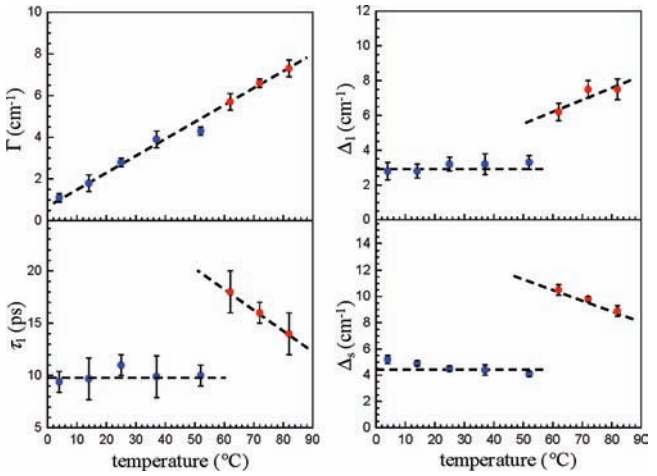


**Figure 8.** Frequency-frequency correlation function parameters plotted against temperature for the native protein (blue data points) and the unfolded protein (red data points). The parameters are the homogeneous line width $\Gamma$, the intermediate time scale decay time constant $\tau_1$, the intermediate time scale amplitude $\Delta_1$, and static component amplitude $\Delta_s$. The dashed lines are aids to the eye. See text for detailed discussion of the parameters. The error bars shown are calculated from error in the fits to the 2D data at each temperature.

are the standard deviations of Gaussian contributions to the absorption line. The total Gaussian component is the convolution of the two Gaussian which has a standard deviation $(\Delta_1^2 + \Delta_s^2)^{1/2}$. The total line shape is Voigt given by the convolution of a Lorentzian with width $\Gamma$ and the total Gaussian component.

The full procedure for calculating the FFCF from CLS and linear spectrum is discussed in detail elsewhere.[49,55] Briefly, the time constants obtained from the exponential fits of CLS give the $\tau_1$ directly as well as $\Delta_s$. The CLS analysis also provides a lower bound on $\Delta_1$, which is at most 15% low. $\Gamma$ and $\Delta_1$ are obtained by simultaneously fitting the linear absorption spectrum and the CLS using the linear and third order response functions. The method has been shown to be robust. For example, the CLS determined FFCF is insensitive to the pulse duration, sloping background absorption, and other factors that can distort the 2D spectra.

Figure 7 displays some of the CLS data. The points are the center line slopes at several temperatures, and the curves are fits to the data with an exponential decay plus an offset. The upper panel contains data taken on the native band, and the lower panel contains data for the unfolded band. The temperature ranges for the native and unfolded data are limited by the difficulty in separating out the CLS for the two bands at temperatures where the bands obscure one another.

As discussed further below, the native 2D data show only a change in the homogeneous component of the dynamic line shape with temperature. This change is manifested by an increasingly large difference from 1 at $T_w = 0$. The $T_w$ dependent portions of the curves are essentially unchanged with temperature. The unfolded 2D spectra also show a change in the homogeneous component of the FFCF with changing temperature. In addition, the shapes of the CLS decay curves are quite different from those obtained from the native 2D spectra, and the unfolded CLS decay curves change shape with temperature.

Figure 8 displays the components of the FFCF obtained from the CLS analysis as a function of temperature. The blue data points are for the native protein, and the red data points are for the unfolded protein. The upper left panel of Figure 8 shows the pure dephasing linewidths vs temperature. This motionally narrowed contribution to the absorption line shape is produced by extremely fast structural fluctuations.[27,56,57] Such structural fluctuations will arise from the motions of small groups on the protein as well as the surrounding water. As the temperature is increased, the pure dephasing line width $\Gamma$ increases linearly. Since $\Gamma = \Delta^2\tau$ and one would expect $\tau$ to become shorter as temperature increases, one way to obtain the observed linear dependence on temperature is for $\tau$ to decrease linearly with temperature while $\Delta$ increases linearly with temperature. The important aspect of the $\Gamma$ vs temperature plot is that the native and unfolded data points fall on the same line. The implication is that the pure dephasing is independent of the state of the protein. This is reasonable if the pure dephasing has major contributions from the water and the motions of small protein molecular groups.

The other components of the FFCF display quite different behavior for the native and unfolded proteins. First consider the native protein data (blue points in Figure 8). The dashed lines through the data points in the $\tau_1$, $\Delta_1$, and $\Delta_s$ plots are horizontal. The plots in Figure 8 show that neither the FFCF decay time and its associated amplitude, $\tau_1$ and $\Delta_1$, nor the static amplitude, $\Delta_s$ have significant temperature dependences. These FFCF parameters are consistent with the lack of a temperature dependence of the native absorptions spectrum's line width and line shape within experimental error. It is possible to draw a slightly increasing line through the $\Delta_1$ data and a slightly decreasing line through the $\Delta_s$ data. However, given the experimental uncertainty, it is not clear that such small temperature dependences are meaningful. If there are such small changes with temperature, it means that some of the dynamics that fall outside of the experimental time window have moved into the experimental time window as the temperature is increased. This behavior would decrease $\Delta_s$ and increase $\Delta_1$. However, the main feature of the native protein FFCF parameters is that they are essentially temperature independent except for the ultrafast fluctuations that give rise to the motionally narrowed pure dephasing.

In contrast to the native protein parameters, $\tau_1$, $\Delta_1$, and $\Delta_s$ for the unfolded protein all display significant temperature dependences (see Figure 8). Unlike the pure dephasing line width $\Gamma$, the unfolded protein's $\tau_1$, $\Delta_1$, and $\Delta_s$ are discontinuous from the values for the folded protein, which are essentially temperature independent. The unfolded protein FFCF decay time, $\tau_1$, decreases with increasing temperature. The corresponding amplitude, $\Delta_1$, increases, while the static component, $\Delta_s$, decreases with increasing temperature.

The results for the unfolded protein have a clear meaning in terms of dynamical time scales. $\Delta_s$ reflects the portion of all of the protein structures that give rise to the inhomogeneous line width and have dynamics that are so slow that they are outside of the experimental time window of ~100 ps. The decrease of $\Delta_s$ means that a portion of the slow dynamics has moved into the experimental time window. Therefore, the very slow structural fluctuations of the protein are becoming faster as the temperature is increased. This change is also reflected by the increase in the value of $\Delta_1$ with increasing temperature. As the temperature is increased, more of the protein's structural fluctuations fall within the ~100 ps experimental time window. The fact that the structural fluctuations of the unfolded protein are becoming faster as the temperature is increased is also shown by the

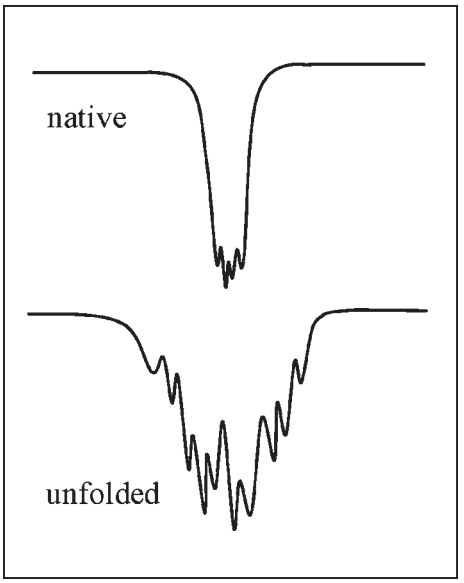


**Figure 9.** Schematic energy landscape diagrams of the native and unfolded structures consistent with the results of the IR experiments. The native protein occupies a narrow energy well with a smaller number of microstates separated by relatively low energy barriers. The thermally unfolded protein has a much broader ensemble of conformational states separated by higher energy barriers.

decrease in $\tau_1$. $\tau_1$ is time constant for the decay of the FFCF, and the time scale for structural fluctuations in the experimental time window that are not so fast that they are motionally narrowed. Therefore, the temperature dependences of $\tau_1$, $\Delta_1$, and $\Delta_s$ all demonstrate that as the temperature increases the structural dynamics of the unfolded protein become faster.

One possibility that would explain the increased rate of structural fluctuations with increasing temperature is that the viscosity of the solvent decreases. Detailed studies have shown that the viscosity dependence of the structural fluctuations of folded proteins as measured by vibrational echo experiments is very mild.[60,61] The vibrational dephasing of CO bound at the active sites of heme proteins increases with decreasing viscosity approximately as $\eta^{1/3}$, where $\eta$ is the viscosity of the solution. Given the small change in viscosity in these experiments with temperature, one would not expect to see a viscosity dependence.[60,61] This is demonstrated by the lack of a temperature dependence, and therefore a viscosity dependence, of the native protein's $\tau_1$, $\Delta_1$, and $\Delta_s$. However, it is possible that an unfolded protein has structural fluctuations that are influenced to a much greater extent by the change in viscosity.

To test for viscosity dependence, the solution viscosities were measured at 62 and 82 °C. The viscosities of the 10 mM cyt *c* solutions are 1.6 cP at 62 °C and 1.3 cP at 82 °C. A small amount of glycerol was added to a protein solution such that at 82 °C it had the same viscosity as the solution without glycerol at 62 °C. The 2D IR vibrational echo experiments were then performed on the 82 °C glycerol-augmented solution. The CLS decay was unchanged by the addition of glycerol to the 82 °C sample. Therefore, a decrease in viscosity with increasing temperature is not responsible for the observed changes in the dynamics of the unfolded protein. Furthermore, the change in temperature itself is not responsible for the change in FFCF parameters for the unfolded state. The homogeneous pure dephasing, $\Gamma$ (see Figure 8) is temperature dependent regardless of the state of the protein, that is, native or unfolded. However, for the other FFCF parameters, the native protein does not show temperature dependence. The data for the native protein covers a change of $k_BT$, where $k_B$ is Boltzmann's constant, of 17%. The data for the unfolded protein spans the range of 62 to 82 °C, which is a change of $k_BT$ of only 6%.

Since the viscosity and the temperature are not responsible for the observed changes going from native to unfolded, the observations must be associated with changes in the structure of the unfolded protein as the temperature is increased. The unfolded protein has a broader range of structures than the native protein as shown by the increased inhomogeneous absorption line width as discussed in Section III.A. This broader range is centered about a different average structure as demonstrated by the shift to a lower frequency of the center of the unfolded absorption band relative to the native band. At the lowest temperature at which the FFCF parameters can be determined for the unfolded protein (62 °C), the unfolded protein $\tau_1$ is slower than it is for the native protein. Thus, in the 100 ps experimental time window, the structural fluctuations of the unfolded protein are slower than those of the native protein. The unfolded protein has a broader range of structures, but the slower interconversions among these structures indicates that there are higher barriers separating distinct structures relative to the ensemble of native structures. A schematic illustration of this difference is given in Figure 9. The unfolded protein is expected to be less ordered and rigid than the native protein. Dynamics of the unfolded protein within the experimental window may involve fluctuations of much larger groups of residues than in the native state. Interconversions among such structures evidently involve higher barriers and slower dynamics. The slowing down of the dynamics is consistent with the idea that the energy landscape becomes more rugged and varied in the unfolded state,[14,62] which corresponds to an increase in the barrier heights separating conformational structures.

## IV. CONCLUDING REMARKS

In this paper, the equilibrium structures and dynamics of the native and thermally unfolded cyt *c* have been examined at various temperatures by linear IR absorption and 2D IR vibrational echo spectroscopic techniques using the heme-ligated CO as the vibrational probe. The temperature dependent absorption area ratio $R_A(T)$ was defined as the ratio of the area under the unfolded band to the sum of the areas of the native and unfolded bands. The temperature dependence of $R_A$ is very similar to the temperature dependent CD data (see Figure 4). The area ratio data display temperature dependent behavior that, by itself, is consistent with two-state unfolding. However, as the temperature is further increased, the unfolded absorption band broadens substantially, and its band center shifts to lower frequency (see Figure 5). The broadening is caused by increased inhomogeneous contributions to the line width that are caused by an expansion in the range of unfolded structures that comprise the unfolded ensemble.

The results of the 2D IR vibrational echo experiments, which yield the FFCF parameters (see Figure 8), show that the native and unfolded proteins have very different dynamics. Both show a temperature dependent increase in the homogeneous component, $\Gamma$, that arises from ultrafast motions that produce a motionally narrowed Lorentzian contribution to the absorption

line. Γ is so narrow at all temperatures that it has almost no influence on the absorption line shape. However, it can be measured with the 2D IR experiments. Starting at low temperature in the native state, Γ increases linearly, and continues to increase in the unfolded state, with the data points falling on the same line. These very fast fluctuations, which have contributions from small groups of the protein and the solvent, are independent of whether the protein is in its native state or unfolded.

In contrast to the homogeneous component, the other FFCF parameters, $\tau_1$, $\Delta_1$, and $\Delta_s$, are very different for the native and unfolded ensembles. $\tau_1$ is the decay time for the FFCF component that falls within the experimental window that extends to ~100 ps. $\tau_1$ can be thought of as the characteristic time scale for protein structural fluctuations on the moderately fast time scale. $\Delta_1$ is the corresponding amplitude (range of frequencies) associated with the intermediate time scale fluctuations and $\Delta_s$ is the amplitude of fluctuations that are so slow (>100 ps) that they fall outside of the experimental time window. The parameters, $\tau_1$, $\Delta_1$, and $\Delta_s$ for the native protein are essentially temperature independent. The lack of temperature dependence of these parameters along with the fact that the native line shape and center frequency do not change with temperature shows that the native protein structure and dynamics are basically independent of temperature over the range studied.

In contrast, $\tau_1$, $\Delta_1$, and $\Delta_s$ for the unfolded protein are all temperature dependent. As the temperature is increased, $\tau_1$ decreases (the dynamics become faster), $\Delta_1$ increases, and $\Delta_s$ decreases. The decrease in $\Delta_s$ and the increase in $\Delta_1$ shows that very slow structural fluctuations are becoming faster and moving into the experimental time window. These changes are caused by changes in the ensemble of protein structures and the barriers that determine the rates of interconversions among structures. The results suggest that the ensemble of the unfolded structures becomes more heterogeneous as unfolding proceeds, and the unfolded ensemble has a very rugged and more varied energy landscape than the native protein as schematically illustrated in Figure 9. These results are consistent with the growing understanding of the unfolded structures of proteins, that is, as an ensemble of more diverse structures compared to the native protein.[1,9,38] In particular, Jimenez et al. have found similar results in horse heart ferricytochrome *c*, a closely related protein, using 3-pulse photon echo peak shift spectroscopy.[10]

Molecular dynamics simulations of these results would be very useful. The experiments presented here can be calculated using MD simulations. Comparison between simulations and these data would provide an important test for the ability of simulations to describe structure and dynamics of proteins that are unfolded to various extents. If the simulations can come reasonably close to reproducing the observed data, then they would provide detailed molecular level insights into the nature of proteins as they become increasingly unfolded.

## ■ ASSOCIATED CONTENT

**Supporting Information.** The Supporting Information contains temperature dependent spectra of the amide region for 10 mM and 3 mM protein samples that demonstrate the absence of protein aggregation. This material is available free of charge via the Internet at http://pubs.acs.org.

## ■ AUTHOR INFORMATION

**Corresponding Author**
fayer@stanford.edu

## ■ ACKNOWLEDGMENT

J.K.C., M.C.T., and M.D.F. thank the National Institutes of Health (2-R01-GM061137-09) for support of this research. We are grateful to Yeonju Kwak for the help with anaerobic sample preparations. M.C.T. also thanks the National Institutes of Health for a post doctoral fellowship. S.E.J.B. and K.L.B. thank the National Institutes of Health (R01-GM63170) for financial support.

## ■ REFERENCES

(1) Dill, K. A.; Shortle, D. *Annu. Rev. Biochem.* **1991**, *60*, 795.
(2) Cho, J. H.; Raleigh, D. P. *Methods Mol. Biol.* **2009**, *490*, 339.
(3) Bren, K. L.; Kellogg, J. A.; Kaur, R.; Wen, X. *Inorg. Chem.* **2004**, *43*, 7934.
(4) Wilkins, D. K.; Grimshaw, S. B.; Receveur, V.; Dobson, C. M.; Jones, J. A.; Smith, L. J. *Biochemistry* **1999**, *38*, 16424.
(5) Jeng, M. F.; Englander, S. W.; Elove, G. A.; Wand, A. J.; Roder, H. *Biochemistry* **1990**, *29*, 10433.
(6) Segel, D. J.; Fink, A. L.; Hodgson, K. O.; Doniach, S. *Biochemistry* **1998**, *37*, 12443.
(7) Hagihara, Y.; Hoshino, M.; Hamada, D.; Kataoka, M.; Goto, Y. *Fold. Des.* **1998**, *3*, 195.
(8) Chattopadhyay, K.; Elson, E. L.; Frieden, C. *Proc. Natl. Acad. Sci. U.S.A.* **2005**, *102*, 2385.
(9) Nettels, D.; Muller-Spath, S.; Kuster, F.; Hofmann, H.; Haenni, D.; Ruegger, S.; Reymond, L.; Hoffmann, A.; Kubelka, J.; Heinz, B.; Gast, K.; Best, R. B.; Schuler, B. *Proc. Natl. Acad. Sci. U.S. A.* **2009**, *106*, 20740.
(10) Jimenez, R.; Romesberg, F. E. *J. Phys. Chem. B.* **2002**, *106*, 9172.
(11) Pace, N. C.; Tanford, C. *Biochemistry* **1968**, *7*, 198.
(12) Chan, H. S.; Dill, K. A. *Annu. Rev. Biophys. Biophys. Chem.* **1991**, *20*, 447.
(13) Chan, H. S.; Dill, K. A. *Proteins: Struct., Funct., Bioinf.* **1998**, *30*, 2.
(14) Frauenfelder, H.; Sligar, S. G.; Wolynes, P. G. *Science* **1991**, *254*, 1598.
(15) Elove, G. A.; Bhuyan, A. K.; Roder, H. *Biochemistry* **1994**, *33*, 6925.
(16) Wain, R.; Redfield, C.; Ferguson, S. J.; Smith, L. J. *J. Biol. Chem.* **2004**, *279*, 15177.
(17) Sasai, M.; Wolynes, P. G. *Phys. Rev. Lett.* **1990**, *65*, 2740.
(18) Weinkam, P.; Zong, C. H.; Wolynes, P. G. *Proc. Nat. Acad. Sci. U.S.A.* **2005**, *102*, 12401.
(19) Travaglini-Allocatelli, C. G., S.; Dubey, V. K.; Borgia, A.; Di Matteo, A.; Bonivento, D.; Cutruzzolà, F.; Bren, K. L.; Brunori, M. *J. Biol. Chem.* **2005**, *280*, 25729.
(20) Massari, A. M.; McClain, B. L.; Finkelstein, I. J.; Lee, A. P.; Reynolds, H. L.; Bren, K. L.; Fayer, M. D. *J. Phys. Chem. B* **2006**, *110*, 18803.
(21) Kim, S.; Chung, J. K.; Kwak, K.; Bowman, S. E.; Bren, K. L.; Bagchi, B.; Fayer, M. D. *J. Phys. Chem. B* **2008**, *112*, 10054.
(22) Filosa, A.; Ismail, A. A.; English, A. M. *J. Biol. Inorg. Chem.* **1999**, *4*, 717.
(23) Filosa, A.; English, A. M. *J. Biol. Inorg. Chem.* **2000**, *5*, 448.
(24) Varhac, R.; Antalik, M.; Bano, M. *J. Biol. Inorg. Chem.* **2004**, *9*, 12.
(25) Latypov, R. F.; Maki, K.; Cheng, H.; Luck, S. D.; Roder, H. *J. Mol. Biol.* **2008**, *383*, 437.
(26) Spiro, T. G.; Wasbotten, I. H. *J. Inorg. Biochem.* **2005**, *99*, 34.
(27) Finkelstein, I. J.; Zheng, J.; Ishikawa, H.; Kim, S.; Kwak, K.; Fayer, M. D. *Phys. Chem. Chem. Phys.* **2007**, *9*, 1533.

(28) Merchant, K. A.; Noid, W. G.; Akiyama, R.; Finkelstein, I.; Goun, A.; McClain, B. L.; Loring, R. F.; Fayer, M. D. *J. Am. Chem. Soc.* **2003**, *125*, 13804.
(29) Merchant, K. A.; Noid, W. G.; Thompson, D. E.; Akiyama, R.; Loring, R. F.; Fayer, M. D. *J. Phys. Chem. B* **2003**, *107*, 4.
(30) Ishikawa, H.; Finkelstein, I. J.; Kim, S.; Kwak, K.; Chung, J. K.; Wakasugi, K.; Massari, A. M.; Fayer, M. D. *Proc. Nat. Acad. Sci. U.S.A.* **2007**, *104*, 16116.
(31) Finkelstein, I. J.; Ishikawa, H.; Kim, S.; Massari, A. M.; Fayer, M. D. *Proc. Natl. Acad. Sci. U.S.A.* **2007**, *104*, 2637.
(32) Thielges, M. C.; Chung, J. K.; Fayer, M. D. *J. Am. Chem. Soc.* **2011**, *133*, 3995.
(33) Finkelstein, I. J.; Goj, A.; McClain, B. L.; Massari, A. M.; Merchant, K. A.; Loring, R. F.; Fayer, M. D. *J. Phys. Chem. B* **2005**, *109*, 16959.
(34) Ishikawa, H.; Kim, S.; Kwak, K.; Wakasugi, K.; Fayer, M. D. *Proc. Nat. Acad. Sci. U.S.A.* **2007**, *104*, 19309.
(35) Ishikawa, H.; Kwak, K.; Chung, J. K.; Kim, S.; Fayer, M. D. *Proc. Nat. Acad. Sci. U.S.A.* **2008**, *105*, 8619.
(36) Pace, C. N.; Scholtz, J. M. In *Protein Structure: A Practical Approach*; Creighton, T. E., Ed.; Oxford: New York, 1997; p 299.
(37) Shortle, D. *Curr. Opin. Struct. Biol.* **1993**, *3*, 66.
(38) Shortle, D.; Meeker, A. K. *Proteins* **1986**, *1*, 81.
(39) Wen, X.; Bren, K. L. *Biochemistry* **2005**, *44*, 5225.
(40) Muga, A.; Mantsch, H. H.; Surewicz, W. K. *Biochemistry* **1991**, *30*, 7219.
(41) Holzbaur, I. E.; English, A. M.; Ismail, A. A. *Biochemistry* **1996**, *35*, 5488.
(42) Park, S.; Kwak, K.; Fayer, M. D. *Laser Phys. Lett.* **2007**, *4*, 704.
(43) Zheng, J.; Kwak, K.; Fayer, M. D. *Acc. Chem. Res.* **2007**, *40*, 75.
(44) Sanbongi, Y.; Igarashi, Y.; Kodama, T. *Biochemistry* **1989**, *28*, 9574.
(45) Senior, W. A.; Verrall, R. E. *J. Phys. Chem.* **1969**, *73*, 4242.
(46) Walrafen, G. E.; Hokmabadi, M. S.; Yang, W. H. *J. Chem. Phys.* **1986**, *85*, 6964.
(47) Phillips, G. N., Jr.; Teodoro, M. N.; Li, T.; Smith, B.; Olson, J. S. *J. Phys. Chem. B* **1999**, *103*, 8817.
(48) Johnson, J. B.; Lamb, D. C.; Frauenfelder, H.; Müller, J. D.; McMahon, B.; Nienhaus, G. U.; Young, R. D. *Biophys. J.* **1996**, *71*, 1563.
(49) Kwak, K.; Park, S.; Finkelstein, I. J.; Fayer, M. D. *J. Chem. Phys.* **2007**, *127*, 124503.
(50) Tokmakoff, A.; Kwok, A. S.; Urdahl, R. S.; Francis, R. S.; Fayer, M. D. *Chem. Phys. Lett.* **1995**, *234*, 289.
(51) Rector, K. D.; Kwok, A. S.; Ferrante, C.; Tokmakoff, A.; Rella, C. W.; Fayer, M. D. *J. Chem. Phys.* **1997**, *106*, 10027.
(52) Golonzka, O.; Khalil, M.; Demirdoven, N.; Tokmakoff, A. *Phys. Rev. Lett.* **2001**, *86*, 2154.
(53) Finkelstein, I. J.; McClain, B. L.; Fayer, M. D. *J. Chem. Phys.* **2004**, *121*, 877.
(54) Bai, Y. S.; Fayer, M. D. *Phys. Rev. B.* **1989**, *39*, 11066.
(55) Kwak, K.; Rosenfeld, D. E.; Fayer, M. D. *J. Chem. Phys.* **2008**, *128*, 204505.
(56) Asbury, J. B.; Steinel, T.; Kwak, K.; Corcelli, S. A.; Lawrence, C. P.; Skinner, J. L.; Fayer, M. D. *J. Chem. Phys.* **2004**, *121*, 12431.
(57) Woutersen, S.; Pfister, R.; Hamm, P.; Mu, Y.; Kosov, D. S.; Stock, G. *J. Chem. Phys.* **2002**, *117*, 6833.
(58) Massari, A. M.; Finkelstein, I. J.; Fayer, M. D. *J. Am. Chem. Soc.* **2006**, *128*, 3990.
(59) Merchant, K. A.; Thompson, D. E.; Xu, Q.-H.; Williams, R. B.; Loring, R. F.; Fayer, M. D. *Biophys. J.* **2002**, *82*, 3277.
(60) Finkelstein, I. J.; Massari, A. M.; Fayer, M. D. *Biophys. J.* **2007**, *92*, 3652.
(61) Rector, K. D.; Jiang, J.; Berg, M.; Fayer, M. D. *J. Phys. Chem. B* **2001**, *105*, 1081.
(62) Onuchic, J. N.; LutheySchulten, Z.; Wolynes, P. G. *Annu. Rev. Phys. Chem.* **1997**, *48*, 545.